Identification of Biological Tissues by Rapid Evaporative Ionization Mass Spectrometry

ARTICLE *in* ANALYTICAL CHEMISTRY · SEPTEMBER 2010

Impact Factor: 5.64 · DOI: 10.1021/ac101283x · Source: PubMed

Anal. Chem. **2010,** *82,* 7343–7350

Identification of Biological Tissues by Rapid Evaporative Ionization Mass Spectrometry

Julia Balog,[†] Tamas Szaniszlo,[†] Karl-Christian Schaefer,[‡] Julia Denes,[‡] Antal Lopata,[§] Lajos Godorhazy,[†] Daniel Szalay,[†] Lajos Balogh,[∥] Laszlo Sasi-Szabo,[⊥] Mikos Toth,[⊗] and Zoltan Takats*[,†,‡,⊗]

Medimass Ltd., Budapest, Hungary, Institute for Inorganic and Analytical Chemistry, Justus Liebig University, Giessen, Germany, Statsoft Ltd., Budapest, Hungary, "Frédéric Joliot-Curie" National Research Institute for Radiobiology and Radiohygiene, Budapest, Hungary, University of Debrecen, Debrecen, Hungary, and Semmelweis University, Budapest, Hungary

The newly developed rapid evaporative ionization mass spectrometry (REIMS) provides the possibility of *in vivo*, *in situ* mass spectrometric tissue analysis. The experimental setup for REIMS is characterized in detail for the first time, and the description and testing of an equipment capable of *in vivo* analysis is presented. The spectra obtained by various standard surgical equipments were compared and found highly specific to the histological type of the tissues. The tissue analysis is based on their different phospholipid distribution; the identification algorithm uses a combination of principal component analysis (PCA) and linear discriminant analysis (LDA). The characterized method was proven to be sensitive for any perturbation such as age or diet in rats, but it was still perfectly suitable for tissue identification. Tissue identification accuracy higher than 97% was achieved with the PCA/LDA algorithm using a spectral database collected from various tissue species. *In vivo*, *ex vivo*, and *post mortem* REIMS studies were performed, and the method was found to be applicable for histological tissue analysis during surgical interventions, endoscopy, or after surgery in pathology.

Rapid and simple identification of biological tissues has long been a problem in the diagnostics and invasive treatment of various forms of cancer. The universally used method for tissue identification is histological examination; however, the histological methods were not developed to provide instant results. The general histological procedure involves fixation, embedding, staining, and sectioning, which usually takes several hours. A further problem is the subjective interpretation of the results. Since histological diagnosis is established based on the visual perception of morphological tissue features, there is a high pathologist-to-pathologist variance of results.[1−9] The above disadvantages become markedly profound when immediate tissue identification is needed during a surgical intervention. For intraoperative histology, a much faster technique, the frozen section method is used.[10−14] Although the frozen section-based investigation takes only 20−30 min, it is still a long time for the patient and the surgeon. Furthermore, the simplified histological processing results in decreased reliability, especially for samples containing high amounts of adipose tissue (e.g., breast cancer).[15]

Histopathological examination nowadays is used in close conjunction with various medical imaging techniques. Malignant tumors are localized preoperatively using positron emission tomography/computed tomography (PET/CT), positron emission tomography/magnetic resonance imaging (PET/MRI), single photon emission computed tomography (SPECT), or sonography, etc.,[16−20] and the histological type of the tumor is determined from

* To whom correspondence should be addressed. Zoltan Takats, Institute for Inorganic and Analytical Chemistry, Justus Liebig University, Schubertstrasse 60, Haus 16, 35392 Giessen, Germany. Fax: +49 641 99 34809. E-mail: Zoltan.Takats@anorg.Chemie.uni-giessen.de.

[†] Medimass Ltd.

[‡] Justus-Liebig-Universität.

[§] Statsoft Ltd.

[∥] "Frédéric Joliot-Curie" National Research Institute for Radiobiology and Radiohygiene.

[⊥] University of Debrecen.

[⊗] Semmelweis University.

(1) Baak, J. P. A.; Langley, F. A.; Talerman, A.; Delemarre, J. F. M. *Gynecol. Oncol.* **1987**, *27*, 166–172.
(2) Ismail, S. M.; Colclough, A. B.; Dinnen, J. S.; Eakins, D.; Evans, D. M. D.; Gradwell, E.; O'Sullivan, J. P.; Summerell, J. M.; Newcombe, R. G. *BMJ* **1989**, *298*, 707–710.
(3) di Loreto, C.; Fitzpatrick, B.; Underhill, S.; Kim, D. H.; Dytch, H. E.; Galera-Davidson, H.; Bibbo, M. *Am. J. Clin. Pathol.* **1991**, *96*, 70–75.
(4) Sørensen, J. B.; Hirsch, F. R.; Gazdar, A.; Olsen, J. E. *Cancer* **1993**, *71*, 2971–2976.
(5) Lanigan, D.; Conroy, R.; Barry-Walsh, C.; Loftus, B.; Royston, D.; Leader, M. *Histopathology* **1994**, *24*, 473–476.
(6) Schapers, R. F. M.; Pauwels, R. P. E.; Wijnen, J. Th. M.; Arends, J. W.; Thunnissen, F. B. J. M.; Coebergh, J. W. W.; Smeets, A. W. G. B.; Bosman, F. T. *Br. J. Urol.* **1994**, *73*, 625–631.
(7) Therkildsen, M. H.; Reibel, J.; Schiødt, T. *Acta Pathol., Microbiol. Immunol. Scand.* **1997**, *105*, 559–565.
(8) Sharkey, F. E.; Sarosdy, M. F. *J. Urol.* **1997**, *157*, 68–71.
(9) Dalton, L. W.; Pinder, S. E.; Elston, C. E.; Ellis, I. O.; Page, D. L.; Dupont, W. D.; Blamey, R. W. *Mod. Pathol.* **2000**, *13*, 730–735.
(10) Jennings, E. R.; Landers, J. W. *Surg. Gynecol. Obstet.* **1957**, *104*, 60–62.
(11) Bauermeister, D. E. *Cancer* **1980**, *46*, 947–949.
(12) Bähr, W.; Stoll, P. *Int. J. Oral Maxillofac. Surg.* **1992**, *21*, 90–91.
(13) Dall'Igna, P.; d'Amore, E. S. G.; Cecchetto, G.; Bisogno, G.; Carretto, E.; Bitetti, S.; Famengo, B.; Alaggio, R. *Pediatr. Blood Cancer* **2010**, *54*, 388–393.
(14) Xu, X.; Chung, J. H.; Jheon, S.; Sung, S. W.; Lee, C. T.; Lee, J. H.; Choe, G. *J. Thorac. Oncol.* **2010**, *5*, 39–44.
(15) Wells, W. A.; Wang, X.; Daghlian, C. P.; Paulsen, K. D.; Pogue, B. W. *Anal. Quant. Cytol. Histol.* **2009**, *31*, 197–207.
(16) Wagner, H. N., Jr.; Conti, P. S. *Cancer* **1991**, *67*, 1121–1128.
(17) Antoch, G.; Vogt, F. M.; Freudenberg, L. S.; Nazaradeh, F.; Goehde, S. C.; Barkhausen, J.; Dahmen, G.; Bockisch, A.; Debatin, J. F.; Ruehm, S. G. *J. Am. Med. Assoc.* **2003**, *290*, 3199–3206.

10.1021/ac101283x
Published on Web 08/03/2010

the tissue sample obtained by biopsy. Although intraoperative application of imaging methods became widespread during the last 2 decades, the imaging methods (especially the intrasurgical setups) do not provide unequivocal differentiation between healthy and cancerous tissue.

The current status of histology and medical imaging techniques invokes a strong need for *in situ*, real-time tissue identification methods. As a response to this need, a number of spectroscopic methods involving *in vivo* labeling or direct spectroscopic investigation of tissues have been developed recently.[21−24] The common scheme of the labeling methods involves the administration of a fluorescent label compound to the patient, which is accumulated by the tumor cells. During the operation, the surgeon identifies the tumor tissue and the proximal metastases (e.g., sentinel lymph node) based on the intensity of the fluorescence. The Achilles-heel of these techniques is the specificity of the label accumulation. Molecularly targeted labels (molecules with specific binding affinity to proteins overexpressed by the tumor cells) can only be used in certain, genetically well-defined cancer types; while nutrient analogues are taken up by any tissue with an elevated level of metabolism (e.g., inflammation). To the present date, no universally applicable label has been developed; however, some highly specific labeling technologies are already in use, for instance in the case of gliomas.[25−27] Besides labeling techniques, direct spectroscopic characterization methods (Raman,[28] Fourier transform-infrared (FT-IR),[29] X-ray scattering[30]) have also been developed for the *in situ* differentiation of malignant tumors from surrounding healthy tissues. Both Raman spectroscopy and Fourier transform-infrared spectroscopy have been successfully applied for *in vivo* analysis of tissues as well as for high-resolution characterization of native frozen tissue sections. One of the main advantages of Raman spectroscopy in this regard is its potential for in-depth analysis, which allows the minimally invasive detection of cancerous tissue features without their surgical exposure. The recent application of Coherent anti-Stokes Raman spectroscopy (CARS)[28] has opened a number of potential new applications for Raman spectroscopic characterization of tissues by providing up to 4 orders of magnitude signal enhancement, 5 mm analysis depth, and improved spectral resolution. Small angle X-ray scattering (SAXS)[30] is an alternative spectroscopic approach for the *in situ* characterization of neoplastic tissues. Although the technique has been introduced recently, differentiation of benign and malignant breast lesions has already been demonstrated.

Mass spectrometry has been used for the investigation of tissues for more than 4 decades.[31,32] The traditional approach involving homogenization, extraction, cleanup, chromatography, and mass spectrometric detection has become the gold-standard method for the quantitative determination of tissue constituents (including drugs and other xenobiotics).[33−36] The advent of desorption ionization methods in the 1980s opened a novel, virtually sample-preparation free approach for the mass spectrometry (MS) investigation of tissue specimens.[37−39] The elimination of sample preparation (especially homogenization) has opened the door to spatially resolved mass spectrometric analysis of tissues, i.e., imaging mass spectrometry.[40,41] The first tissue imaging studies (matrix-assisted laser desorption ionization (MALDI), secondary ion mass spectrometry (SIMS)) already found spectra to be highly tissue specific. Even subtle histological differences, such as the level of dedifferentiation (grade) of malignant tumors were successfully detected by imaging MALDI.[42−44] An important advantage of mass spectrometric imaging is the objectivity of the information. While in histology the tissue parts are identified based on the visual perception of morphological features, mass spectrometry provides numerical data which makes user-independent identification feasible. In spite of the above advantages, imaging mass spectrometry has not become widespread in tissue analysis, mainly due to the poor spatial resolution (compared to that of the optical methods), the time demand of imaging (several hours per sample without any possible way for multiplexing), and the costly instrumentation.

Imaging MS techniques, like histology, require thin sections of tissue specimens mounted on slides. Similarly to immunohistochemical methods, imaging MS determines the spatial distribution of a molecular species in tissue sections, however not only 1 but 50−500 species in a single imaging experiment. However, the application area of imaging mass spectrometry does not exceed the limits of histology and does not provide remedy for the problems of *in situ*, real-time tissue identification.

Although a number of mass spectrometric techniques (including desorption electrospray ionization (DESI), direct analysis in real time (DART), atmospheric pressure solids analysis probe

(18) von Schulthess, G. K. *Mol. Imaging Biol.* **2004**, *6*, 183–187.
(19) Gaa, J.; Rummeny, E. J.; Seemann, M. D. *Eur. J. Med. Res.* **2004**, *9*, 309–312.
(20) Delbeke, D.; Schoder, H.; Martin, W. H.; Wahl, R. L. *Semin. Nucl. Med.* **2009**, *39*, 308–340.
(21) Hoffman, R. M. *Nat. Rev. Cancer* **2005**, *5*, 796–806.
(22) Frangioni, J. V. *J. Clin. Oncol.* **2008**, *26*, 4012–4021.
(23) Kosaka, N.; Ogawa, M.; Choyke, P. L.; Kobayashi, H. *Future Oncol.* **2009**, *5*, 1501–1511.
(24) Themelis, G.; Yoo, J. S.; Soh, K. S.; Schulz, R.; Ntziachristos, V. *J. Biomed. Opt.* **2009**, *14*, 064012-9.
(25) Stummer, W.; Stocker, S.; Wagner, S.; Stepp, H.; Fritsch, C.; Goetz, C.; Goetz, A. E.; Kiefmann, R.; Reulen, H. J. *Neurosurgery* **1998**, *42*, 518–526.
(26) Stummer, W.; Novotny, A.; Stepp, H.; Goetz, C.; Bise, K.; Reulen, H. J. *J. Neurosurg.* **2000**, *93*, 1003–1013.
(27) Stepp, H.; Beck, T.; Beyer, W.; Pongratz, T.; Sroka, R.; Baumgartner, R.; Stummer, W.; Olzowy, B.; Mehrkens, J. H.; Tonn, J. C.; Reulen, H. J. In *Photonic Therapeutics and Diagnostics*; Bartels, K. E., Eds.; SPIE: Bellingham, WA, 2005; pp 547−557.
(28) Krafft, C.; Dietzek, B.; Popp, J. *Analyst* **2009**, *134*, 1046–1057.
(29) Petibois, C.; Deleris, G. *Trends Biotechnol.* **2006**, *24*, 455–462.
(30) Fernandez, M.; Keyrilainen, J.; Serimaa, R.; Torkkeli, M.; Karjalainen-Lindsberg, M. L.; Tenhunen, M.; Thomlinson, W.; Urban, V.; Suortti, P. *Phys. Med. Biol.* **2002**, *47*, 577–592.
(31) Snedden, W.; Parker, R. B. *Anal. Chem.* **1971**, *43*, 1651–1656.
(32) Han, X. L.; Gross, R. W. *J. Lipid Res.* **2003**, *44*, 1071–1079.
(33) Bachmann, C.; Colombo, J.-P.; Berüter, J. *Clin. Chim. Acta* **1979**, *92*, 153–159.
(34) Kim, H. Y.; Yergey, J. A.; Salem, N., Jr. *J. Chromatogr., A.* **1987**, *394*, 155–170.
(35) Gelpí, E. *J. Chromatogr., A.* **1995**, *703*, 59–80.
(36) Want, E. J.; Cravatt, B. F.; Siuzdak, G. *ChemBioChem* **2005**, *6*, 1941–1951.
(37) Tangrea, M. A.; Wallis, B. S.; Gillespie, J. W.; Gannot, G.; Emmert-Buck, M. R.; Chuaqui, R. F. *Expert Rev. Proteomics* **2004**, *1*, 185–192.
(38) Caldwell, R. L.; Caprioli, R. M. *Mol. Cell. Proteomics* **2005**, *4*, 394–401.
(39) Cooks, R. G.; Ouyang, Z.; Takats, Z.; Wiseman, J. M. *Science* **2006**, *311*, 1566–1570.
(40) Burnum, K. E.; Frappier, S. L.; Caprioli, R. M. *Annu. Rev. Anal. Chem.* **2008**, *1*, 689–705.
(41) Lee, T. G.; Park, J.-W.; Shon, H. K.; Moon, D. W.; Choi, W. W.; Li, K.; Chung, J. H. *Appl. Surf. Sci.* **2008**, *255*, 1241–1248.
(42) Djidja, M.-C.; Claude, E.; Snel, M. F.; Scriven, P.; Francese, S.; Carolan, V.; Clench, M. R. *J. Proteome Res.* **2009**, *8*, 4876–4884.
(43) Pevsner, P. H.; Melamed, J.; Remsen, T.; Kogos, A.; Francois, F.; Kessler, P.; Stern, A.; Anand, S. *Biomarkers Med.* **2009**, *3*, 55–69.
(44) Kang, S.; Shim, H. S.; Lee, J. S.; Kim, D. S.; Kim, H. Y.; Hong, S. H.; Kim, P. S.; Yoon, J. H.; Cho, N. H. *J. Proteome Res.* **2010**, *9*, 1157–1164.

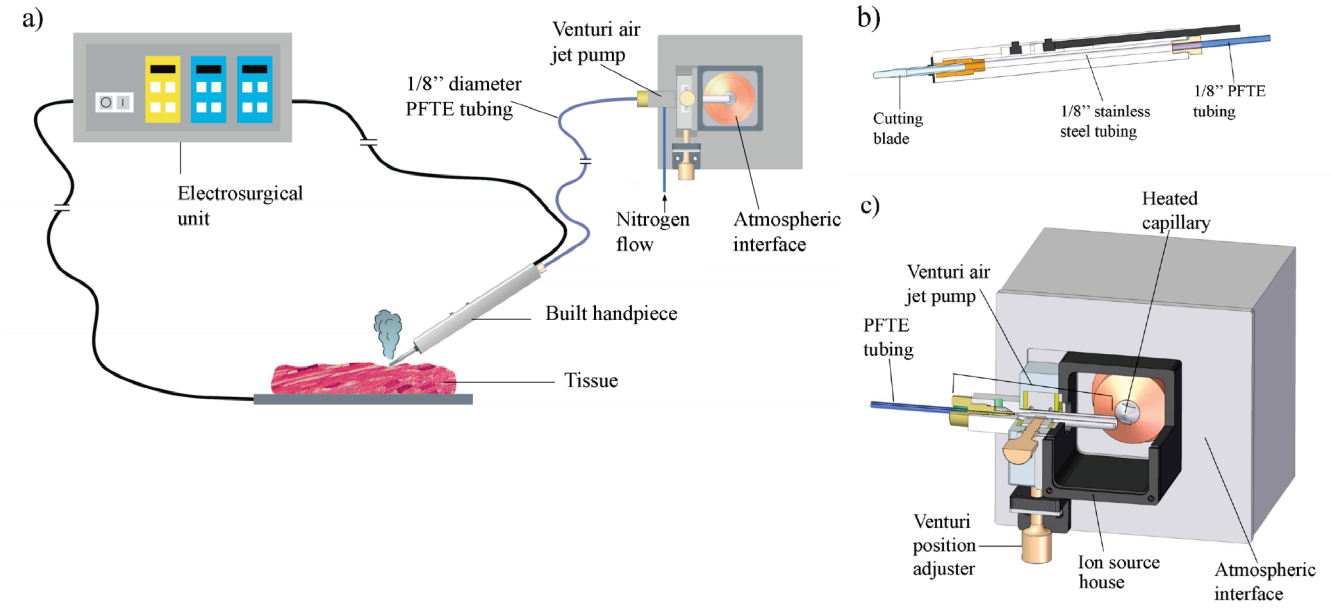

Figure 1. Surgical ion source and transfer setup: (a) schematic figure of ion transfer from the tissue to the atmospheric interface; (b) custom built electrosurgical handpiece; and (c) mounting of the Venturi air jet pump on the atmospheric interface of the LTQ/LCQ mass spectrometers.

(ASAP), etc.) not requiring sample preparation have been recently developed,[45] tissue analysis using these methods is either not demonstrated yet (however, it is possible in case of DART and desorption atmospheric pressure chemical ionization (DAPCI)) or require frozen tissue sections (DESI). The basis of the present study was the discovery that surgical methods employing thermal ablation (electrosurgery and infrared laser surgery) produce large amount of tissue-originated gaseous ions.[46] Since the corresponding mass spectra were found to be similar to those obtained by DESI, SIMS, or MALDI, this combination (i.e., electrosurgery/mass spectrometry) provides a basis for developing the desired *in situ*, real-time tissue identification method. In the present study, our objective was to characterize this group of methods termed rapid evaporative ionization mass spectrometry and develop it to the level of medical applicability.

EXPERIMENTAL SECTION

Ion Source/Transfer Setups. REIMS experiments were performed using two, distinctively different experimental setups. One setup was designed to comply with the requirements of surgical interventions, while the second one is more of a traditional imaging ion source for desorption ionization experiments. The surgical ion source and ion transfer setup is depicted in Figure 1. The ionization of the sample (i.e., vital biological tissues) takes place at the surgical site, in close conjunction with the electrosurgical dissection of the tissues. The electrosurgical dissection was carried out using a commercially available Radiosurg 2200 (Meyer-Haake, Wehrheim, Germany) electrosurgical unit and a custom built electrosurgical handpiece and cutting electrode (Figure 1a). The most important feature of the cutting electrode is that the actual cutting blade is embedded into an open, $^1/_8$ in. diameter stainless steel tubing. The stainless steel tubing is connected to a 2 m long, $^1/_8$ in. diameter PTFE tubing through the handpiece (Figure 1b). The described vent line is used for the evacuation of the aerosol containing gaseous ions from the surgical site and the transmission of the ions to the distant mass spectrometer by a home-built Venturi gas jet pump (Figure 1c). Although there are commercially available devices for the evacuation of toxic surgical smoke, these devices were found to be unsuitable for ion transfer due to large dead volumes and the dilution of the samples.

Electrosurgery is defined as a group of tissue manipulation methods employing high-frequency electric current for tissue ablation, cutting, and coagulation. In the case of electrosurgical intervention, current is directly applied onto vital tissues, where thermal damage occurs exclusively via the dissipation of electric energy due to their nonzero impedance.

The ionization process was associated with the formation of charged droplets (of both polarities) during tissue evaporation. Contribution of the rf arc (observed between the electrode and tissue surface) to formation of ions observed is considered to be minimal (vide infra).

The Venturi gas jet pump was driven by nitrogen or zero air introduced at 4 bar nominal pressure. The Venturi pump was mounted into the source housing in the orthogonal position relative to the heated capillary inlet of an LCQ Deca XP Max quadrupole ion trap mass spectrometer (Thermo Finnigan Llc., San Jose, CA) or an Orbitrap Discovery Fourier transform mass spectrometer (Thermo Fisher Scientific Inc., Bremen, Germany). A home-built source housing was designed for compatibility with the Thermo Ion Max ion source platform. The orthogonal position of the Venturi pump was chosen to minimize contamination of the atmospheric interface (for further details see the Results and Discussion). The REIMS imaging ion source (Figure S-1 in the

(45) Van Berkel, G. J.; Pasilis, S. P.; Ovchinnikova, O. *J. Mass Spectrom.* **2008**, *43*, 1161–1180.
(46) Schäfer, K. C.; Denes, J.; Albrecht, K.; Szaniszlo, T.; Balog, J.; Skoumal, R.; Katona, M.; Toth, M.; Balogh, L.; Takats, Z. *Angew. Chem., Int. Ed.* **2009**, *48*, 8240–8242.

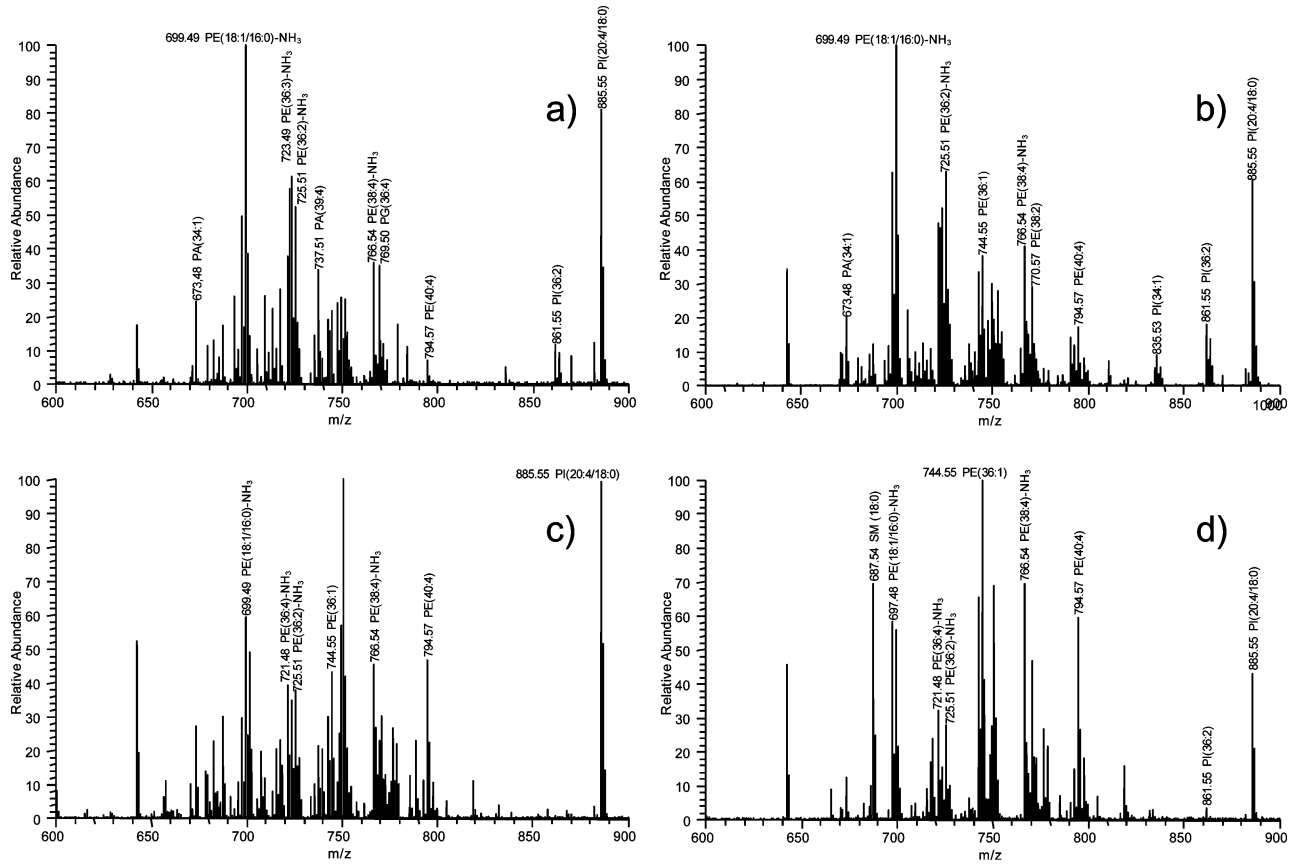

Figure 2. Negative ion spectra of vital animal tissues obtained using different thermal evaporation methods: (a) porcine kidney medulla, CO_2 laser ablation; (b) porcine kidney medulla, electrosurgical dissection; (c) canine stomach mucosa, CO_2 laser ablation; and (d) canine stomach mucosa, electrosurgical dissection.

Supporting Information) was designed for spatially controlled REIMS data collection using *ex vivo* or *post mortem* tissue specimens.

Samples. Food-grade porcine organs were used for performance testing of the devices. The effect of nutritional factors was studied in the rat model. Canine *in vivo* and *ex vivo* data was acquired from dogs with spontaneous tumors from veterinary oncology praxis. Human samples were obtained from the Institute of Pathology, University of Debrecen. All required ethical permissions were obtained for both the animal experiments and the collection/analysis of human samples (for further details on the samples see the Supporting Information).

Data Analysis. Mass spectra were collected in single stage MS, negative mode, in the mass range 600−900 m/z, unless otherwise stated. Spectral data was reduced using a 1 m/z bin size in the case of the QIT data and a 0.01 m/z bin size in the case of the Orbitrap data. Data were subjected to principal component analysis (PCA) and in some cases linear discriminant analysis (LDA) using a home-built software package. Prior to PCA analysis, spectra were normalized by dividing each point of the spectra by the average intensity. This is necessary to get all spectra to the same order, correcting the measurement mistakes. Before using NIPALS algorithm for PCA, we subtract the average from each variable, converting the means to zero. Results obtained by the home-built software were validated using STATISTICA (StatSoft, CA) software. The identification of the spectra was performed using a spectral database. The method of identification comprises the definition of a PCA space, the localization of the spectral class data in a 60-dimensional LDA space (based on the PCA space) and the determination of the tissue type by squared Mahalanobis distances to classes created by the LDA.

Leave 20%-out cross-validation was used to assign the number of significant principal components. In each case the spectra left out were classified with LDA and the number of misclassified spectra were counted. The best classification was achieved with 50−70 components (2−3 mistakes from 1500−2000), and there was a small overfitt above 70 components (3−5 mistakes). These data suggested the use of 60 components in the discriminant analysis.

RESULTS AND DISCUSSION

Rapid evaporative ionization mass spectrometry[46] in general covers all methods which involve the rapid, thermally induced disintegration of bulk, condensed phase samples yielding gaseous ions. In this sense, there are a number of different ways of implementation depending on the method of heating. Potential heating methods include Joule-heating, contact heating, and radiative heating. The latter group includes even infrared-laser ablation, and indeed, spectra obtained by IR-LA (or laser desorption ionization) show high similarity to those obtained by the electrosurgical Joule heating method, which is used throughout the present study (Figure 2). Although there are a number of potential applications of REIMS ranging from environmental analysis through process monitoring to liquid chromatography−mass spectrometry (LC−MS) interfacing, the most significant application remains the analysis of intact, even vital biological

Table 1. Identified Species in REIMS Spectra

		tissue specificity
	Positive Ion Mode	
phosphatidyl-cholines (PC)	16:0, 16:1, 18:1, 18:2, 20:4, 20:2, 20:3, 22:6	no
phosphatidyl-serines (PS)	16:0, 16:1, 18:0, 20:4	no
phosphatidyl ethanolamines (PE)	14:0, 16:0, 16:1, 18:1, 18:2, 20:4, 20:2, 20:3 22:6	no
sphingomyelins (SM)	18:0, 18:1, 20:4, 22:6	yes (nervous tissue)
triglycerides (NH_4^+ adducts)	16:0, 16:1, 18:1, 18:2, 20:4, 20:2, 20:3 22:6	no
	Negative Ion Mode	
fatty acids	2:0, 3:0, 4:0, 8:0, 8:1, 10:0, 10:1, 12:0, 12:1, 14:0, 14:1, 16:0, 16:1, 18:0, 18:1, 18:2, 20:2, 20:3, 20:4, 22:6	no
phosphatidyl ethanolamines (PE)	14:0, 16:0, 16:1, 18:1, 18:2, 20:4, 20:2, 20:3 22:6	no
phosphatidyl ethanolamines-NH_3 (PE-NH_3)	identical to PE	no
phosphatidyl serines (PS)	16:0, 18:1, 18:0	no
phosphatidyl inositols (PI)	16:0, 16:1, 18:0, 18:1, 18:2, 20:4, 22:6	no
sulfatides	16:0, 18:1, 20:4	yes (brain white matter)
plasmalogens	16:0, 18:1	no/yes (invasive ductal carcinoma)
phosphatidic acids	16:0, 18:1, 18:0	yes (adenocarcinoma)
eicosanoids	PGE_2, PGI_2	yes (inflammation)
lysophospholipids	16:0, 16:1, 18:1, 18:2	yes (necrosis, inflammation)
cardiolipins	18:1, 18:2, 18:3	yes (myocardium)
cholesterol		no
heme		no

tissues. The unique features of the REIMS methods which make them suitable for intact biological tissue analysis include the lack of sample preparation, no requirement on the sample geometry, and the fact that these methods are already used for tissue manipulation, although not for analysis but for surgical dissection. An obvious result of this latter feature is that the instrumentation for ionization is commercially available and fully approved even for *in vivo* applications.

The REIMS spectra of intact biological tissues, independently from the method of heating, feature predominantly protonated or deprotonated ions of various lipids and their primary thermal degradation products (Figure 2). The list of identified species is summarized in Table 1. Peak identification was carried out by accurate mass measurement and MS/MS experiments.

The instrumental settings influencing the ionization and the ion collection were investigated in detail. The most important physical factor for REIMS is the rate of heating; however, the determination of this factor is not straightforward for radiative or Joule heating. Since the heating rate is largely determined by the heating power setting of the electrosurgical generator or the surgical laser, the effect of this setting was studied in detail. Regarding relative overall signal intensity, there is a well-defined optimum setting for the heating power, thus, most likely also for the heating rate. The increase of the ionization efficiency at higher heating power is associated with the higher evaporation rate of the sample and the more efficient disintegration of the bulk tissue material. The decline of the ionization efficiency at extreme high power settings was attributed to thermal degradation effects caused by the higher evaporation temperature. The thermal degradation of phosphoethanolamines via the loss of ammonia was also enhanced with increasing power setting (Figure 3), together with the visible carbonization of the tissues. An interesting feature of the REIMS process is the dependence of spectral characteristics on the atmospheric interface settings of the mass spectrometer. While the dependence of the overall signal intensity on the heated capillary temperature setting is similar to that of electrospray ionization, the atmospheric interface potential settings (heated capillary potential and tube lens potential) have no measurable effect on signal intensity or on the ion distribution in the spectra. This phenomenon was associated with the presence of an extremely large amount of partially charged aerosol in the atmospheric interface and the fact that REIMS produces charged particles of both polarities, similarly to sonic spray[47] or MALDI.[48]

The phospholipid distribution in various tissues is generally considered to be tissue-specific, based on phosphorus-NMR data;[49−52] however, the biochemical background of this phenomenon has not been fully clarified. The spectra obtained from different types of tissue by REIMS are characteristically different (Figure 2). The reproducibility and the general nature of this fingerprint character is better demonstrated by principal component analysis (PCA). Spectra from various canine organs were distinctly separated even using only the first three PCA components (Figure 4). Although visual representation is not possible, data points obtained from more than 60 different tissue types show complete separation using 60-dimensional PCA. An interesting feature of this phenomenon is that practically no tissue-specific marker lipid components were observed. All identified lipid components were detected in >80% of the investigated tissue types; hence, only the distributions and not the individual molecules are responsible for the tissue specificity of the REIMS spectra.

Since one of the most significant components of the phospholipid distribution patterns is the acyl-chain distribution within the individual phospholipid classes, the spectra were expected to show strong dependence on nutritional fatty acid intake. This assumption was tested using a rat model consisting of three experimental groups, which were fed three different diets. The fatty acid composition of the three feeds is shown in Table S-1 in the

(47) Hirabayashi, Y.; Hirabayashi, A.; Koizumi, H. *Rapid Commun. Mass Spectrom.* **1999**, *13*, 712–715.
(48) Dashtiev, M.; Wafler, E.; Rohling, U.; Gorshkov, M.; Hillenkamp, F.; Zenobi, R. *Int. J. Mass Spectrom.* **2007**, *268*, 122–130.
(49) Meneses, P.; Para, P. F.; Glonek, T. *J. Lipid Res.* **1989**, *30*, 458–461.
(50) Metz, K. R.; Dunphy, L. K. *J. Lipid Res.* **1996**, *37*, 2251–2265.
(51) Merchant, T. E.; Kasimos, J. N.; Vroom, T.; de Bree, E.; Iwata, J. L.; de Graaf, P. W.; Glonek, T. *Cancer Lett.* **2002**, *176*, 159–167.
(52) Srivastava, N. K.; Pradhan, S.; Gowda, G. A. N.; Kumar, R. *NMR Biomed.* **2010**, *23*, 113–22.

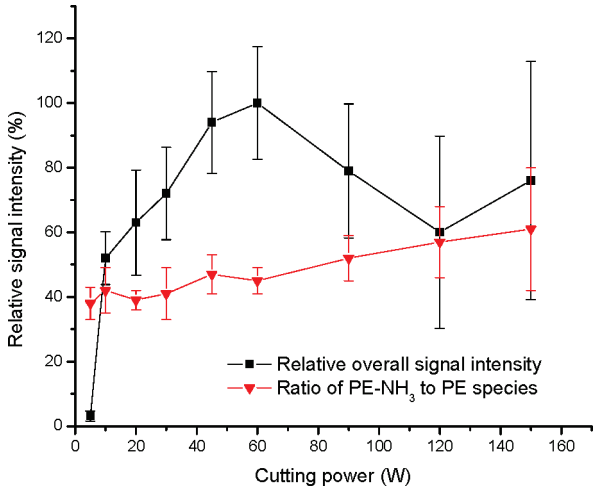

Figure 3. Dependence of overall signal intensity and the extent of phosphoethanolamine degradation on the heating power of the electrosurgical device.

Supporting Information. During the 10 week experiment, different organs of animals from each experimental group were investigated *in vivo* under phenobarbital anesthesia. *In vivo* REIMS spectra of various tissues showed practically no dependence on the nutritional fatty acid intake. The sole exception was the myocardial tissue (Figure 5), presumably due to the elevated fatty acid metabolism of the heart,[53] but the spectral changes did not affect the identification of the tissue. The rate of correct classification was not higher if the spectra of the three diets were separated than in the combined database (Tables S-2 and S-3 in the Supporting Information). The age of the animals also resulted in differences in the spectral patterns (Table S-4 in the Supporting Information), it also had no effect on tissue identification. We can conclude that nutritional and age factors have a negligible effect; hence, the method has a real potential for tissue identification in the case of human or veterinary patients living on an arbitrary diet.

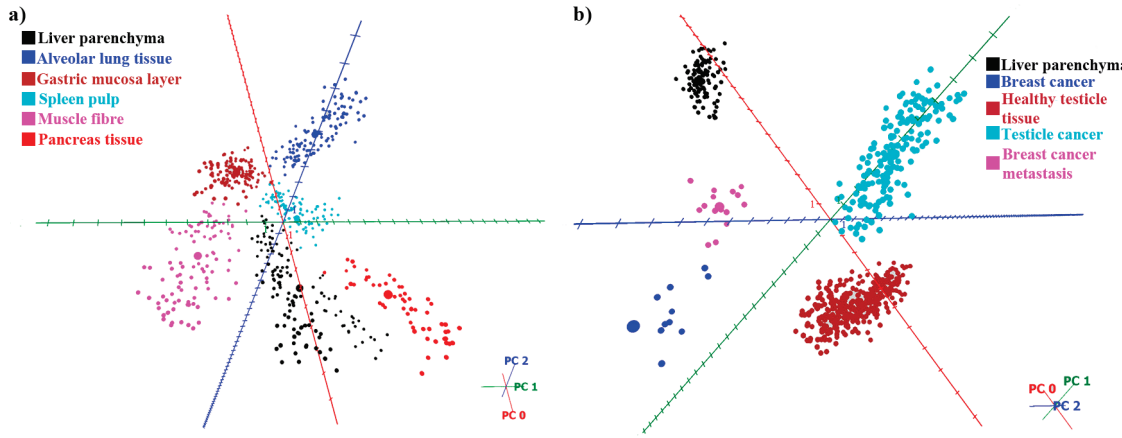

Figure 4. Three-dimensional PCA visualization of spectra obtained from different canine organs: (a) six healthy *ex vivo* canine organs and (b) *ex vivo* healthy and cancerous tissues. The three-dimensional PCA explains 46.02% of the variance in the former and 60.59% in the latter case. In comparison, 60-dimensional PCA (used for identification) explains 79.09 and 83.93%, respectively.

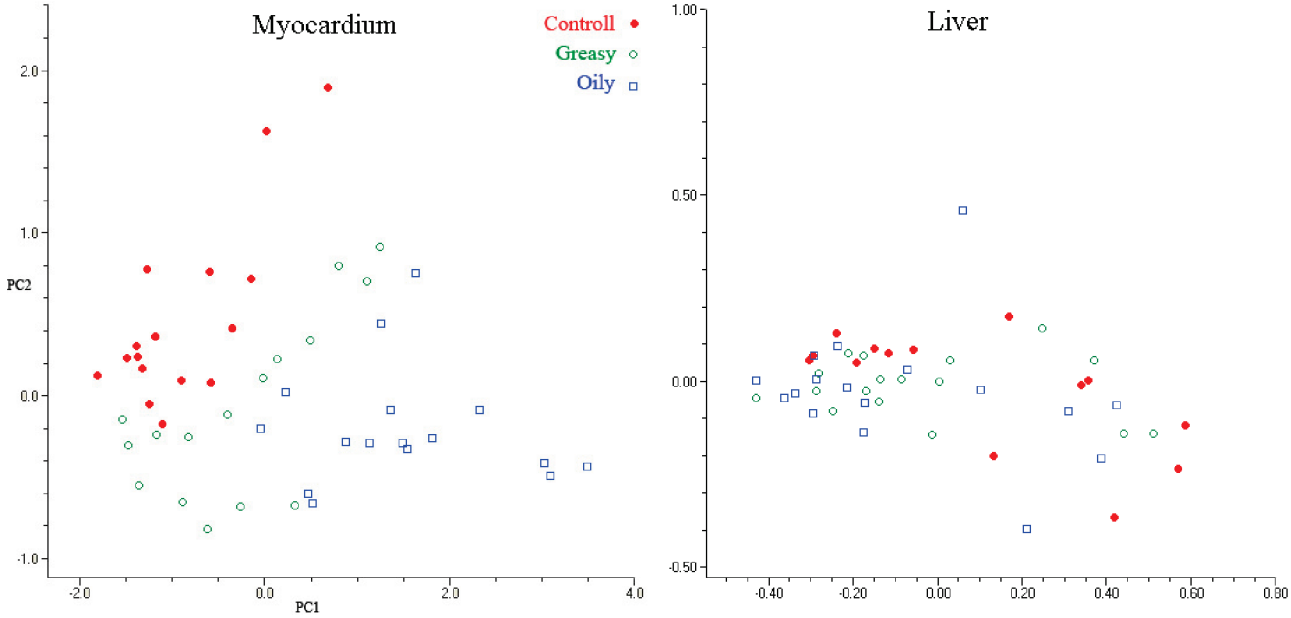

Figure 5. Effect of diet on myocardial and liver parenchymal spectra in rat. In the liver, the different fatty acid intakes had no effect, while the myocardial spectra were differentiated in accordance with the diet, but the spectral changes did not affect the identification of the tissue. Two-dimensional PCA explains 43.67% and 37.42% of the variance, respectively.

As it was pointed out in the introduction, fast and accurate identification of the tissues is most relevant in the diagnostics and surgical therapy of malignant tumors. In order to utilize REIMS-based tissue identification in surgery (or diagnostics), distant sampling technologies had to be developed. Ion transfer was implemented using a Venturi air jet pump and a 2 m long flexible tubing.[54,55] Experimental setup is shown in Figure 1a. Since REIMS ionization does not require any dc potential on the samples, an ion population comprising both positive and negative ions is formed, which allows the utilization of polymer tubing for ion transfer. In the present case, static charge buildup of the tube is avoided via neutralization by counterions formed during the REIMS process, thus flexible polymer tubing is freely applicable.

Minimizing the residence time of ions in the tubing is preferred for multiple reasons including neutralization kinetics and practical applicability. Neutralization occurs via the recombination of the positive and negative ions formed in parallel during the REIMS process. With the use of the depicted setups, sampling efficiencies far lower than 100% were achieved; hence in order to achieve maximum sensitivity, both gas flow rate and linear velocity had to be maximized. The effect of the Venturi inlet pressure on the evacuation flow rate was investigated, results are shown in the Supporting Information (Figure S-2).

From the practical point of view of the surgeons, an analysis should be achieved in few seconds, by minimizing the ion transfer and data analysis time. This quasi real-time evaluation of the data was achieved by creating databases prior to the surgical interventions and comparing real-time spectra to the database entries. A given database consists of at least 50 spectra of all tissue types which can theoretically be sampled during the intervention. All database spectra were recorded in the 600−900 m/z mass range at unit resolution. The 300-dimensional data vectors were noise-filtered and reduced to 60 dimensions via principal component analysis, and the differentiation of the organs is carried out with 60-dimensional linear discriminant analysis (LDA), still prior to the operation. Real-time classification of spectra was performed by using the precalculated 60 LDA parameters of the database entries and classifying the spectra in this LDA space via calculating squared Mahalanobis distances. This way the time-consuming calculation of PCA and LDA parameters is done before the operation and only the fast distance calculation is performed online. A critically important parameter of tissue identification is the data accumulation time for the individual data points. On one hand, the signal-to-noise ratio improves with longer data collection times, on the other hand, dissection of one histologically/anatomically homogeneous tissue feature takes a limited amount of time. Hence, in order to acquire meaningful spectra originated from an at least anatomically homogeneous sample, data collection time is limited to 1 s. Fortunately the increase of data collection time in the case of the database entries also enhances the accuracy of identification (Figure S-3 in the Supporting Information).

The described system was tested in tumor resection surgeries of canine subjects carrying spontaneous tumors. The handpiece depicted in Figure 1b was proven to be fully functional as an electrosurgical device. No adverse effect of the depicted aerosol evacuation system to the surgical performance was observed. Figure 6a shows the use of a REIMS-compatible electrosurgical handpiece during a canine tumor surgery.

It is important to point out that the formation of tissue originated gaseous ions occurs independently from the mass spectrometric analysis, hence the mass spectrometer is only a passive element in the experimental setup. REIMS analysis of the tissues is utilized in two, fundamentally different ways. In the so-called alerting mode the ionic species in the surgical aerosol are continuously analyzed and the mass spectrometric system gives continuous feedback on the nature of the tissue being dissected. Screenshot of the graphical user interface of our software taken during surgery is shown in Figure 6c. Whenever the result of the real-time spectral identification refers to the presence of a malignant proliferation or the identification fails, the system gives audiovisual alerting to surgeon. The alternative way of utilization is the microprobe mode, when the tissue features of interest are sampled actively for the purpose of identification. From the perspective of mass spectrometric tissue identification, the main difference between the two modes is the data accumulation time for individual spectra. While in alerting mode data is accumulated for 0.5−1 s, in microprobe mode the data for one spectrum is accumulated as long as the button on the handpiece is held down. In order to demonstrate the accuracy of intraoperational tissue identification, results obtained from individual sampling points (Figure 6a) are shown in a 3D PCA plot (Figure 6b).

Mechanistic Considerations. REIMS spectra of tissues feature protonated or deprotonated molecular ions of various lipid-type species ranging from fatty acids to cardiolpins or cerebrosides. Similarly, REIMS analysis of aqueous solutions of amino acids, drug molecules, or peptides also yields protonated or deprotonated ions. Alkali metal and ammonium adducts have also been observed; however, radical ions have not been detected, not even in those cases when the ionization was performed directly at the atmospheric inlet of the instrument. As it has been pointed out in the Supporting Information of an earlier communication,[46] the ion formation mechanism can be associated either with the formation of charged, aqueous droplets (similarly to sonic spray) when the tissue is thermally disintegrated or with the, often visible, radio frequency electric discharge between the electrode and tissue surface. On the basis of experimental results, it was concluded that the ion formation mechanism most likely follows the former scenario.[46]

In order to further elucidate the ion formation mechanism, alternative tissue evaporation methods not involving electric discharge were investigated. Laser ablation was found to yield highly similar spectra shown in Figure 2. CO_2 laser ablation is considered to be a purely thermal process (no electronic excitation of molecules is involved), hence the spectral similarity suggests that ion formation observed during electrosurgery follows a similar pathway. Thermal evaporation of homogenized tissue was also performed via contact heating with similar results. (Figure S-4 in the Supporting Information). The only significant difference in this case was the less pronounced ammonia loss of phosphatidylethanolamine species. This observa-

(53) Stein, O.; Stein, Y. *Biochim. Biophys. Acta, Spec. Sect. Lipid Relat. Subj.* **1963**, *70*, 517–530.
(54) Zhou, L.; Yue, B. F.; Dearden, D. V.; Lee, E. D.; Rockwood, A. L.; Lee, M. L. *Anal. Chem.* **2003**, *75*, 5978–5983.
(55) Hawkridge, A. M.; Zhou, L.; Lee, M. L.; Muddiman, D. C. *Anal. Chem.* **2004**, *76*, 4118–4122.

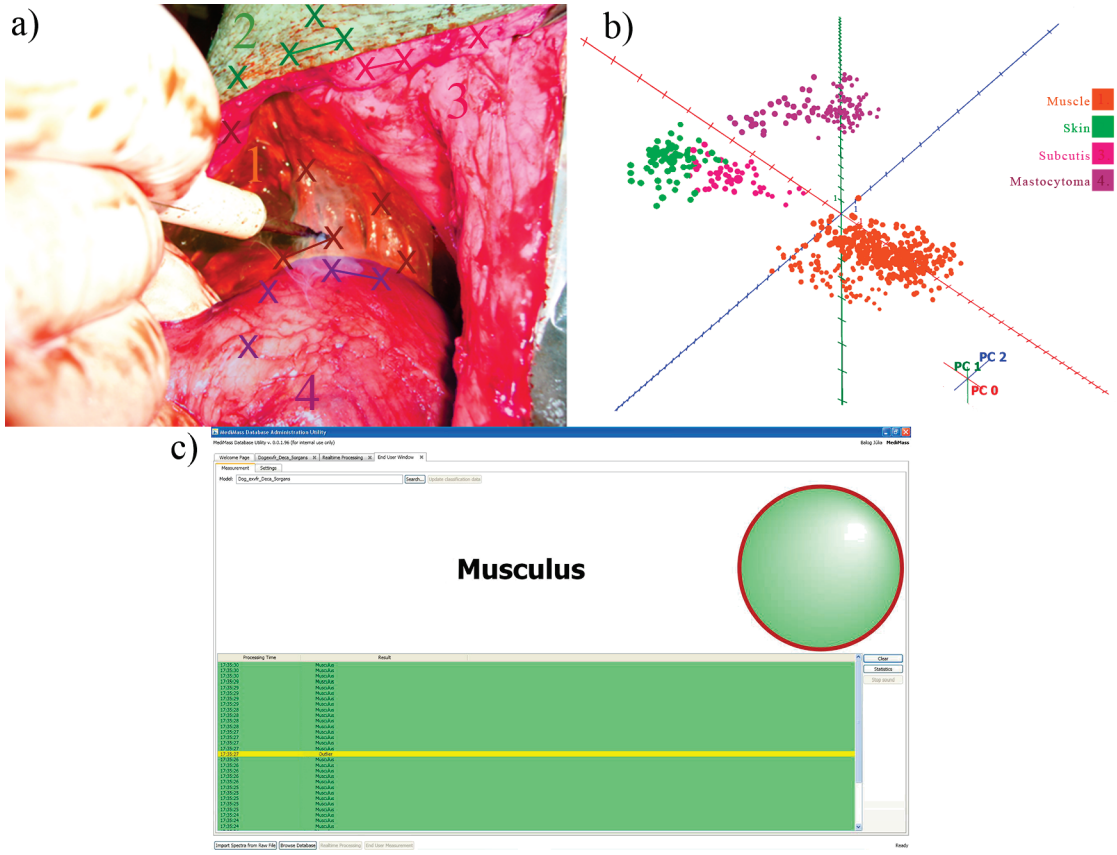

Figure 6. REIMS analysis during canine oncological surgery: (a) picture has been taken during the surgical dissection of a grade III mastocytoma in canine, different type of tissues were colored for better understanding, samples were taken from the marked sections; (b) three-dimensional principal component analysis of the spectra taken from the marked places (the three-dimensional PCA in this case explains 52.07% of the variance, while 60-dimensional PCA explains 81.22%); (c) screenshot of the realtime software during surgery.

tion gives further support for the assumed thermally induced disintegration-based ion formation scenario. Further assumptions on ionization methods are discussed in the Supporting Information.

CONCLUSIONS

The described methods provide not only a potential solution for *in situ*, real-time tissue identification but also increase the significance of well established mass spectrometric tissue analysis methods especially of those capable of tissue imaging. Although the correlation between REIMS and MALDI (or other desorption methods, such as DESI or SIMS) phospholipid spectra is not deciphered yet, combination of REIMS with any of these desorption ionization techniques will result in a complex tissue analysis methodology which provides comparable data in the operating room and histopathology lab. This latter feature is practically not achievable even using the whole current arsenal of histology.

REIMS analysis is especially promising for tumor resection surgeries where not an entire anatomical part of the body is removed. These include resection of brain tumors, tumors of the gastrointestinal tract, liver tumors, lung cancer, thyroid cancer, breast cancer. The method can possibly be combined with the diagnostic procedure in the case of endoscopic interventions, e.g., colonoscopy. In these cases all suspicious tissue features can be tested and the decision on their resection can be made immediately. Similar approach is feasible in the case of cervical cancer or dermatological lesions.

ACKNOWLEDGMENT

The work was funded by the European Research Council under Starting Grant scheme (Contract No. 210356) and the Hungarian National Office for Research and Technology under Jedlik Ányos Grant scheme (JEDIONKO Grant).

SUPPORTING INFORMATION AVAILABLE

Additional information as noted in text. This material is available free of charge via the Internet at http://pubs.acs.org.

Received for review May 25, 2010. Accepted July 21, 2010.

AC101283X